Determination of the Light-Induced Degradation Rate of the Solar Cell Sensitizer N719 on TiO_2 Nanocrystalline Particles

Farahnaz Nour-Mohhamadi,[†] Sau Doan Nguyen,[†] Gerrit Boschloo,[‡,§] Anders Hagfeldt,[‡,§] and Torben Lund*[,†]

Department of Life Sciences and Chemistry, Roskilde University, DK-4000, Denmark, and Department of Physical Chemistry, Uppsala University, Box 579, SE-72123 Uppsala, Sweden

Received: May 26, 2005; In Final Form: September 28, 2005

The oxidative degradation rate, k_{deg}, of the solar cell dye $(Bu_4N^+)_2[Ru(dcbpyH)_2(NCS)_2]^{2-}$, referred to as **N719** or $[RuL_2(NCS)_2]$, was obtained by applying a simple model system. Colloidal solutions of **N719**-dyed TiO_2 particles in acetonitrile were irradiated with 532-nm monochromatic light, and the sum of the quantum yields for the oxidative degradation products $[RuL_2(CN)_2]$, $[RuL_2(NCS)(CN)]$, and $[RuL_2(NCS)(ACN)]$, Φ_{deg}, was obtained at eight different light intensities in the range of 0.1−16.30 mW/cm^2 by LC−UV−MS. The Φ_{deg} values decreased from 3.3×10^{-3} to 2.0×10^{-4} in the applied intensity range. By using the relation $k_{deg} = \Phi_{deg} k_{back}$ and back electron-transfer reaction rates, k_{back}, obtained with photoinduced absorption spectroscopy, it was possible to calculate an average value for the oxidative degradation rate of **N719** dye attached to TiO_2 particles, $k_{deg} = 4.0 \times 10^{-2}$ s^{-1}. The stability of **N719** dye during solar cell operation was discussed based on this number, and on values of the electron-transfer rate between $[Ru^{(III)}L_2(NCS)_2]$ and iodide ion that are available in the literature.

Introduction

Nanocrystalline dye-sensitized titanium dioxide solar cells (nc-DSSC), developed by O'Regan and Grätzel,[1] have attracted significant attention because of their high solar-to-electric power conversion efficiency and low cost compared to those of silicon solar cells.[2−4] The best performing dye-sensitized solar cells reported to date are based on a nanocrystalline TiO_2 film sensitized with ruthenium polypyridyl complexes and having an overall light-to-electricity conversion efficiency $\eta \sim 10-12\%$ and excellent stability.[5−7] For practical applications, the long-term stability of the nc-DSSC is very important. The stability of various cell components has been investigated by several research groups and much information has been obtained about the factors and mechanisms that control their stability and efficiency.[6−17] On the basis of accelerated illumination tests, some authors have estimated DSSC lifetimes to be between 5 and 10 years under outdoor illumination conditions,[11,12] while others have claimed that such long cell lifetimes are not achievable.[8,9] The most important single component in the nc-DSSC is the sensitizer dye, and the long-term stability and efficiency of the cells is thus related to its stability. Most investigations have focused on the ruthenium dye $[RuL_2(NCS)_2]$ (L = 4,4′-dicarboxylic acid 2,2′-bipyridyl) and its tetrabutylammonium salt, referred to as **N3** and **N719**, respectively.

The operating principle of a nanocrystalline dye-sensitized titanium dioxide solar cell with **N3** dye as the sensitizer is as shown in eqs 1−3.

$$TiO_2|Ru^{(II)}L_2(NCS)_2 + h\nu \rightarrow TiO_2|Ru^{(II)}L_2(NCS)_2^* \quad (1)$$

$$TiO_2|Ru^{(II)}L_2(NCS)_2^* \rightarrow TiO_2 + e^-|Ru^{(III)}L_2(NCS)_2^+ \quad (2)$$

$$TiO_2|Ru^{(III)}L_2(NCS)_2^+ + I^- \rightarrow TiO_2|Ru^{(II)}L_2(NCS)_2 + I^\bullet \quad (3)$$

The ruthenium dye, which is anchored to the TiO_2 surface by bidentate coordination,[18] is excited by the incoming light (eq 1) and transformed to the oxidized form by an ultrafast electron injection process from the excited state to the conduction band of the TiO_2 semiconductor (eq 2).[19−20] The chemistry of the photoanode is completed by the regeneration of the starting complex by an electron transfer from the mediator I^- (eq 3).[21,22,27b] To achieve 20 years of solar cell operation under outdoor illumination conditions, the ruthenium dye sensitizer should be able to sustain more than 10^8 cell cycles and the rate of possible side reactions should be as low as possible. The sensitizer dye may in principle degrade from its ground state, S, excited state, S*, or oxidized state, S^+. The *cis*-$[Ru^{(II)}L_2(NCS)_2]$ complex has been shown to be thermally very stable[23] and the injection rate of eq 2 so fast ($k_{inj} > 1 \times 10^{13}$ s^{-1}) that side reactions initiated from the exited state can be ruled out. Therefore, the most likely degradation pathway occurs from the Ru(III) oxidized state. The instability of $[Ru^{(III)}L_2(NCS)_2]^+$ is apparent from the irreversible voltammograms of the complex[10,24] and from the fact that electrochemical oxidation of $[RuL_2(NCS)_2]$ in acetonitrile does not produce the blue color ($\lambda = 740$ nm) characteristic of a $Ru^{(III)}$ complex.[25] The stability of the dye during solar cell operation is therefore dependent on the rate of regeneration of the $Ru^{(II)}$ dye (eq 3) compared with the rate of degradation of the $Ru^{(III)}$ complex (eq 4).

* Address correspondence to this author. Fax: 45-46743011. E-mail: tlund@ruc.dk.
[†] Roskilde University.
[‡] Uppsala University.
[§] Current address: Department of Chemistry, Royal Institute of Technology, SE-10044 Stockholm, Sweden.

10.1021/jp052792v CCC: $30.25
Published on Web 11/05/2005

$$TiO_2|Ru^{(III)}L_2(NCS)_2^{+} \xrightarrow{k_{deg}} \text{degradation products} \quad (4)$$

$$TiO_2 + e^-|Ru^{(III)}L_2(NCS)_2^{+} \xrightarrow{k_{back}} TiO_2|Ru^{(II)}L_2(NCS)_2 \quad (5)$$

Knowledge of the oxidation products of $[Ru^{(II)}L_2(NCS)_2]$ and the oxidative degradation rate, k_{deg}, are essential parameters for the prediction of the long-term stability of the dye under solar cell operation. Though several reports have focused on the degradation products,[10,26] to our knowledge no one has previously attempted to obtain the degradation rate, k_{deg}.

The aim of this research is to obtain the degradation rate, k_{deg}, of $[Ru^{(III)}L_2(NCS)_2]^+$ attached directly onto the nanocrystalline TiO_2 particles. The complicated solar cell system is replaced by a simpler model system based on a stirred suspension of **N719**-dyed TiO_2 particles in acetonitrile irradiated by monochromatic light ($\lambda = 532$ nm). As iodide is absent in this experiment, oxidized dye molecules will recombine with electrons injected into the TiO_2 particles (eq 5) or take part in a degradation reaction, as illustrated in Figure 1.

The total amount of degradation products, $\sum n_{deg}$, generated during the illumination of dyed TiO_2 particles is quantitatively monitored by high-pressure liquid chromatography (HPLC) coupled to a UV−vis detector and a mass spectrometer (MS). The quantum yield of all degradation products, Φ_{deg}, may be calculated according to eq 6, where N_a is the number of absorbed photons. The quantum yield depends on the competition between the degradation reaction (eq 4) and back electron-transfer reaction (eq 5) and may be related to the rate of these reactions through eq 7.

$$\Phi_{deg} = \sum n_{deg}/N_a \quad (6)$$

$$\Phi_{deg} = \frac{k_{deg}}{k_{deg} + k_{back}} \sim k_{deg}/k_{back}; \qquad k_{back} \gg k_{deg} \quad (7)$$

The rate of the back electron-transfer reaction has been measured by laser flash photolysis and photoinduced absorption (PIA), and values in the range of 10^3 to 10^6 s^{-1} have been reported.[27−29] Considering the light intensity dependence of the back electron-transfer reaction rate,[29] in order to use this rate as a basis for calculating the rate of the degradation reaction, it is necessary to obtain k_{back} under the same light intensity and experimental conditions as used in the photolysis experiments. In this work we obtained back electron-transfer reaction rates at different light intensities by means of PIA measurements.

Experimental Section

Materials. The bistetrabutylammonium salt of the complex *cis*-bis(isothiocyanato)bis(2,2′-bipyridyl-4,4′-dicarboxylato)ruthenium(II), with the trade name Ruthenium 535-bis TBA, and referred to as **N719**, was obtained from Solaronix. HPLC-grade acetonitrile (Merck) was dried by passing the solvent through a column of activated neutral alumina particles. The actinometer Aberchrome 540, (*E*)-α-(2,5-dimethyl-3-furylethylidene)isopropylidene succinic anhydride, was purchased from Aberchromics Ltd., Wales.

The dye degradation experiments were performed by two different methods described below.

Method 1: *Preparation of Dye-Covered Nanocrystalline TiO_2 Films*. A colloidal TiO_2 suspension was prepared by mixing Degussa P25 titanium dioxide (∼2 g) with ∼20 mL of absolute ethanol. Small glass balls ($d = 5$ mm) were added and the mixture was ground by shaking overnight. Nanocrystalline TiO_2 films were prepared by spraying the colloidal TiO_2 suspension onto nonconductive glass plates (length 7 cm, width 1.5 cm), using an airbrush (Olympos Airbrush model HP-100C with nozzle diameter of 0.3 mm), followed by heating the plates under an air atmosphere for 30 min at 450 °C. The titanium dioxide coverage of the plates was between 16 and 25 mg (1.52−2.38 mg/cm^2). Dye coating was made by soaking the TiO_2 glass plates in **N719** dye solution in absolute ethanol (6×10^{-5} M) overnight and at room temperature. All the dyed plates were stored in absolute ethanol in the dark.

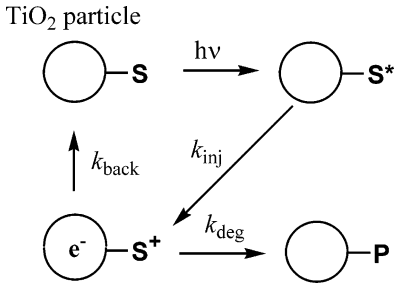

Figure 1. Schematic representation of the model system used in the photolysis experiments.

Photolysis Experiments by Method I. The degradation experiments were carried out in a UV cuvette prepared as described below. The dyed titanium dioxide particles prepared as thin films were removed from the glass plates as small aggregates and transferred into a cuvette ($1 \times 1 \times 3$ cm^3) capped with an airtight membrane. The cuvette was filled with acetonitrile (3 mL) and then the oxygen was removed by argon gas (99.995%, $O_2 < 10$ ppm) bubbling for about 20 min. During illumination the colloidal solution was magnetically stirred. In all photolysis experiments the cuvettes were placed in the black box of the photon-counting device. The active area of the cuvette exposed to the light was approximately 2 cm^2.

Dye Extraction Procedure. At the end of every photolysis experiment the dyed titanium dioxide particles were transferred into a test tube. After centrifugation, most of the solvent was removed with use of a Pasteur pipet. The dye on the remaining TiO_2 particles was extracted by treatment with a mixture of aqueous NaOH (0.1 M, 2 mL) and absolute ethanol (1 mL). After centrifugation, the red solution containing the dye and its degradation products was decanted and, after acidifying with 15 μL of concentrated formic acid, was analyzed with LC−UV−MS. Control experiments showed that **N719** and its photodegradation products were stable in 0.10 M NaOH at room temperature.

Preparation of the Standard Solutions. Standard solutions of **N719** were prepared in absolute ethanol (1×10^{-5} to 1×10^{-4} M) and the LC−MS chromatograms obtained. An external standard curve was constructed and used to quantify the amount of degradation products in the photolysis experiments. The quantitative analysis of photolysis mixtures was based on the approximation that **N719** dye and its degradation products would all have the same sensitivity in the MS detector.

Method II: *Preparation of Dye-Covered TiO_2 Particles.* Degussa P25 TiO_2 (600 mg) was magnetically stirred in 250 mL of an **N719** dye solution ([**N719**] $= 6.06 \times 10^{-5}$ mol/L) in absolute ethanol. After 24 h all of the dye molecules in the solution were completely adsorbed onto the surface of the titanium dioxide particles. Centrifuging an aliquot of this mixture resulted in a colorless liquid above the pink solid (dyed TiO_2), confirming the complete adsorption of the dye onto the TiO_2 particles. After removing the colorless liquid by rotary evapora-

tion, the red-colored nanocrystalline TiO_2 particles were transferred into a brown bottle that was wrapped in aluminum foil and stored in the dark.

Preparation of the Dyed TiO_2 Colloidal Solution. The dyed nanocrystalline TiO_2 powder (12 mg of dye with 0.304 μmol of **N719**) was placed into a cuvette containing 3 mL of dry acetonitrile. The mixture was degassed with a flow of argon gas for 20 min. After degassing, a "homogeneous" stable dyed TiO_2 colloidal solution was obtained by sonification of the cuvette for 1 h.

Photolysis Experiments. The cuvette containing the dyed colloidal TiO_2 solution was placed into the black box of a photon-counting device. The sample was irradiated with continuous laser light (532 nm) of known intensity (0.1−16 mW/cm^2) for the duration needed to obtain the predefined light doses. Six photolysis experiments with light doses of $(1-6) \times 10^5$ counting numbers (1×10^5 counting numbers $= 3.18 \times 10^{-5}$ mol of photons) were performed at each laser light intensity. After irradiation, the dyed TiO_2 colloidal solution was transferred into a round-bottom flask and the acetonitrile was removed by means of rotary evaporation.

The degradation products from the photolysis experiments that were still bound to the TiO_2 particles were extracted by means of treatment with a solution comprised of 2 mL of 0.1 M NaOH and 1 mL of ethanol. The red extract in the flask was transferred into a clean test tube and then centrifuged. After the white TiO_2 particles were removed, the red liquid was transferred to another test tube and 15 μL of formic acid was added. The acidified solution was then transferred into an HPLC vial and analyzed with LC−UV.

Instrumentation. *HPLC−UV/Vis−MS Equipment.* The LC−MS instrument was equipped with a UV diode array detector with a 5-cm flow cell in series with an MS detector. The HPLC instrument was a TSP Spectra System equipped with an AS3000 auto sampler, a P4000 gradient pump, a vacuum degasser, and a UV 6000 LP diode array detector. Separation was performed with a linear gradient program starting with 100% A (5% acetonitrile + 94% water + 1% formic acid) ending after 21.6 min with 100% B (acetonitrile). Elution with 100% B continued for a further 10 min, followed by a return to 100% A after a further 5 min. The flow rate was 0.2 mL/min. The analytical column was a 50-mm Xterra MS RP C18 column from Waters with an i.d. of 2.1 mm. The mass detector was an LCQ-Deca ion-trap instrument from ThermoFinnigan equipped with an electrospray ionization interface (ESI) run in positive mode. A positive potential (+4.5 kV) was applied to the silica needle, while the other details of the setup were as follows: discharge current 19−20 mA, capillary voltage 23 V, capillary temperature 350 °C, tube lens offset 5 V, and sheath gas (N_2) and auxiliary gas (N_2) 78 and 45 arbitrary units, respectively. UV−vis absorptions were recorded between 400 and 600 nm. The ion trap was run in the data-dependent MS scan mode. The scan event was obtained in the 400−800 *m*/*z* interval. The parent mass list was *m*/*z* 643.1, 648.1, 674.9, and 706, while the reject mass list was *m*/*z* 547, 569, 585, 591, 613, 629, 636, and 592. The isolation *m*/*z* width was 6, the normalized collision energy was 35, the activation time was 30 ms, and minimum signal required 10^5 counts. Xcalibur 1.2 LCQ software controlled the chromatographic and mass spectrometric analysis.

Light Sources. Three light sources were used. Low-intensity light was generated by an Oriel, 300-W tungsten−halogen lamp in combination with a 435-nm cutoff filter and a 525 ± 5-nm interference filter. The light intensity of this source was 0.2 mW. Approximately two-thirds of the cuvette (2 cm^2) was illuminated, corresponding to an intensity of 0.1 mW/cm^2. A second light source was a slide projector equipped with a 250-W halogen lamp in combination with an IR water filter and a UV−vis 525 ± 5-nm interference filter. The intensity of this source was 1.07 mW or ∼0.54 mW/cm^2. The third light source was a 532-nm laser with a light intensity of 16.3 mW/cm^2. The intensity of the laser light could be reduced by using neutral density filters (Oriel).

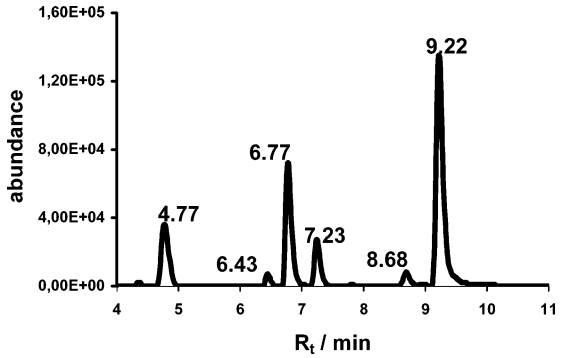

Figure 2. LC−UV chromatogram of a dye extract obtained after laser light illumination of a colloidal solution of **N719**-dyed TiO_2 particles in deoxygenated acetonitrile, prepared using method II: laser light intensity, 2.86 W/cm^2; excitation wavelength, 532 nm; mol of absorbed photons, 1.91×10^{-4} mol.

Photon-Counting Device. A homemade photon-counting device was used in the photolysis experiments. The device consisted of a black box, a cuvette holder, and a light-splitting system in which 90% of the light was directed toward the sample and 10% to a photodiode. The electrical response of the diode was monitored and integrated electronically.

Actinometry Experiment. Aberchrome 540 in toluene (5 mM) was used as a chemical actinometer in the visible region to calibrate the photon-counting device. The Abercrome solution (3 mL) was first irradiated with UV light until a red-colored solution of absorbance ∼2 was obtained. Then, the red solution was exposed to the visible light source, i.e., the 532-nm laser light, and the absorbance decrease of the solution was obtained as a function of the counting number obtained from the photon-counting device.

Photoinduced Absorption Spectroscopy. The photoinduced absorption (PIA) apparatus has been described elsewhere.[29] Briefly, a 1.0-mm path-length cuvette containing the dyed TiO_2 sample was illuminated with chopped light from a 532-nm He−Ne continuous wave laser. Resulting absorption changes at 800 nm were probed with light from a filtered tungsten−halogen lamp (λ > 715 nm), using a monochromator, a Si-detector, and a lock-in amplifier set at the chopping frequency (range 400 to 4 Hz). Neutral density filters were used to attenuate the laser beam. Time constants were obtained with a nonlinear, least-squares fit of the frequency domain data.

Results and Discussion

Identification of the Dye Degradation Products. Figure 2 shows the LC−UV chromatogram of a dye extract obtained from a representative laser irradiation experiment performed on a pink colloidal solution of **N719**-dyed TiO_2 particles prepared following method II. In all the photolysis experiments that involved applying different light sources and intensities, six peaks were observed in the chromatograms. The degradation products observed in the photolysis experiments were similar to those observed as resulting from the electrochemical oxidation of **N719** in acetonitrile and dimethylformamide.[26] The UV and MS spectra of these oxidative degradation products have recently been described,[26] and a list of λ_{max} and important *m*/*z* values of

TABLE 1: Data of Retention Times, Absorption Maxima, and Characteristic *m/z* Values of N719 and Its Degradation Products Obtained from Degradation Experiments Performed on N719-Dyed TiO_2 Nanocrystalline Particles in Acetonitrile

complex	formula[a]	r_t/min	characteristic *m/z* values	λ_{max}
1	$[RuL_2(NCS)_2]$	9.22	706, 648	525
2	$[RuL_2(NCS)(SCN)]$	8.70	706, 648	521
3	$[RuL_2(CN)_2]$	4.78	643	470
4	$[RuL_2(NCS)(CN)]$	6.77	675,648	497
5	$[RuL_2(NCS)(ACN)]$	7.25	689, 648	481
6	$[RuL_2(NCS)(H_2O)]$	6.45	667, 648	512

[a] L = 4,4′-dicarboxylic acid 2,2′-bipyridyl. ACN = CH_3CN.

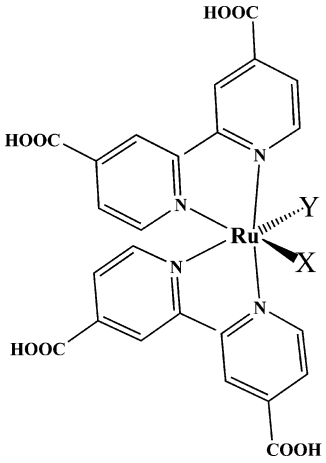

	X	Y
1	**NCS**	**NCS**
2	**SCN**	**NCS**
3	**CN**	**CN**
4	**NCS**	**CN**
5	**NCS**	**CH_3CN**
6	**NCS**	**H_2O**

Figure 3. Structure of **1**−**6**.

the products is shown in Table 1**.** The structures of the starting dye molecule and its degradation products are shown in Figure 3.

Compound **1** is the main component of the acidified dye extracts. This product is the fully protonated form of the unreacted starting **N719** complex. Compound **2** is the S/N thiocyanate isomer of **1**. A sample of the **N719** starting material contains approximately 5% of the complex, with one S- and one N-bound thiocyanate ligand. Compounds **3**−**5** are the main degradation products. Compound **4** is characterized by its mass spectrum, which shows ruthenium isotope patterns around the ions, *m/z* 675, $[RuL_2(NCS)(CN) + H]^+$, and *m/z* 648, $[RuL_2(NCS)]^+$. The latter ion is formed by the elimination of an $NCS^{\bullet -}$ radical from the molecular ion. Product **4** is produced through an internal oxidation mechanism in the complex, initiated by the electron-transfer process between the NCS^- ligand and the $Ru^{(III)}$ center.[7] Complex **3** is characterized by its yellow color (λ_{max} = 470 nm) and a ruthenium isotope pattern around the ion, *m/z* 643, which may be assigned to the ion $[RuL_2(CN)_2 + H]^+$. Interestingly, compound **3** was also observed in the electrochemical oxidation of **N719** in dimethylformamide, but not from the electrolysis of **N719** in acetonitrile.[26] Product **3** is likely produced by a further photooxidation of **4**. Compound **5** is characterized by its *m/z* value of 689, corresponding to the $[RuL_2(NCS)(ACN)]^+$ ion. The complex was also observed in the electrolysis of **N719** in acetonitrile, and is believed to be formed via a solvent-dependent mechanism.[26] The mass spectrum of the peak at R_t = 6.45 min (**6**) showed a low-intensity ruthenium isotope pattern around the *m/z* value of 667, which may be assigned to the $[RuL_2(NCS)(H_2O) + H]^+$ ion. Compound **6** was observed as an impurity (<1%) in the starting material**.** The concentration of **6** was constant during the photolysis experiments, and the presence of **6** was therefore explained as an **N719** impurity and not a product produced during the photolysis.

Quantum Yield Determination. Table 2 shows the results of six laser photolysis experiments with a laser light intensity of 9.58 mW/cm^2 along with the moles of absorbed photons in each experiment. Degradation products **3**−**5** were quantified from the LC−UV chromatograms by dividing the area of each product peak by the total peak areas of compounds **1**−**5** and multiplying this ratio by n_{dye} , the starting number of moles of **N719** dye in the cuvette. In these calculations it is assumed that compounds **1**−**5** all have the same extinction coefficient at their respective visible absorption maxima. Parts a and b of Figure 4 show the evolution of degradation products **3**, **4**, and **5** and the total amount of these three products as a function of the moles of absorbed photons. The results presented in Figure 4a,b were obtained by using method II with a laser light intensity of 9.58 mW/cm^2 and by using method I with a light intensity of 0.10 mW/cm^2, respectively. As observed from Figure 4a,b, reasonably straight lines are obtained for all three products. The intercepts with the *y*-axis of **3** and **5** are nearly zero, as expected, whereas an intercept is observed for **4**, indicating an initial degradation of **N719** to **4** before the start of photolysis. The origin of this initial degradation is unknown; however, impurity defects in the Degussa P25 nanoparticles may be responsible for the observed oxidative thermal degradation. The slopes of the lines representing the sum of the three oxidative degradation products, **3**−**5**, in Figure 4a,b are equal to the total quantum yield of oxidative degradation products at the respective intensities. The quantum yields of degradation at 9.58 and 0.10 mW/cm^2 were $(3.1 \pm 0.4) \times 10^{-4}$ and $(3.2 \pm 0.2) \times 10^{-3}$, respectively. The lower the light intensity, the higher the value of Φ_{deg}.

Determination of k_{back}. Photoinduced absorption measurements[29] were performed on a colloidal solution of **N719**-dyed TiO_2 particles prepared by using method I and laser light intensities in the range of 0.5 to 5 mW/cm^2. Magnetic stirring of the solution was eliminated by using ultrasound waves to make a stable colloidal solution during the experiment. The back electron-transfer time, τ_{back}, was extracted from the frequency dependence of the PIA signals. Figure 5 shows τ_{back} as a function of the incident light intensity, *I*. τ_{back} decreases with the increasing intensity of the excitation laser light. The back electron-transfer rate appears to follow a power-law dependence on the light intensity (λ = 532 nm); see eq 8.

$$k_{back} = \frac{1}{\tau_{back}} = \frac{1}{0.0127 I^{-0.4043}} = 78.74 I^{0.4043} \qquad (8)$$

Determination of k_{deg}. The oxidative degradation rate of the dye, k_{deg}, may be calculated from the back electron-transfer reaction rate, k_{back}, and the total quantum yield of all degradation products, according to eq 7. A complication arises, however, due to the change in the light intensity throughout the length of the light pathway inside the cuvette. This results from the light absorption by the dyed TiO_2 particles and causes the light intensity to decrease continuously throughout the length of the cuvette. As discussed in the previous paragraph, k_{back} depends on the excitation light intensity (see eq 8), and therefore will decrease from a high value, $k_{back}(I_0)$, at the front of the cuvette (l = 0 cm), to a value near zero at l = 1 cm. The uncorrected degradation rate constant, k^u_{deg}, may be calculated from eq 9. This rate is too fast compared to the actual degradation rate, because $k_{back}(I_0)$ is too high compared to a weighted average of k_{back}. The correction factor, f_c, defined as in eq 10, is derived from the mathematical

TABLE 2: Data from Photolysis Experiments with Laser Intensity of 9.58 mW/cm²

compd	R_t/min	expt 1[a]	expt 2[a]	expt 3[a]	expt 4[a]	expt 5[a]	expt 6[a]
3	4.78	2.05×10^{-9}	2.37×10^{-9}	4.67×10^{-9}	3.32×10^{-9}	6.78×10^{-9}	9.39×10^{-9}
4	6.78	1.72×10^{-8}	2.20×10^{-8}	2.27×10^{-8}	3.39×10^{-8}	3.71×10^{-8}	3.53×10^{-8}
5	7.25	5.72×10^{-9}	1.21×10^{-8}	1.17×10^{-8}	1.89×10^{-8}	2.70×10^{-8}	2.54×10^{-8}
2	8.70	1.93×10^{-8}	2.23×10^{-8}	2.20×10^{-8}	2.06×10^{-8}	1.94×10^{-8}	1.83×10^{-8}
1	9.22	2.61×10^{-7}	2.39×10^{-7}	2.30×10^{-7}	2.14×10^{-7}	2.03×10^{-7}	1.97×10^{-7}
n_{dye}		3.14×10^{-7}	3.06×10^{-7}	3.01×10^{-7}	3.04×10^{-7}	3.04×10^{-7}	2.95×10^{-7}
n_{DP}		2.50×10^{-8}	3.65×10^{-8}	3.91×10^{-8}	5.61×10^{-8}	7.09×10^{-8}	7.01×10^{-8}
n_{photon}		3.18×10^{-5}	6.36×10^{-5}	9.54×10^{-5}	1.27×10^{-4}	1.59×10^{-4}	1.91×10^{-4}

[a] All numbers in the columns are in moles.

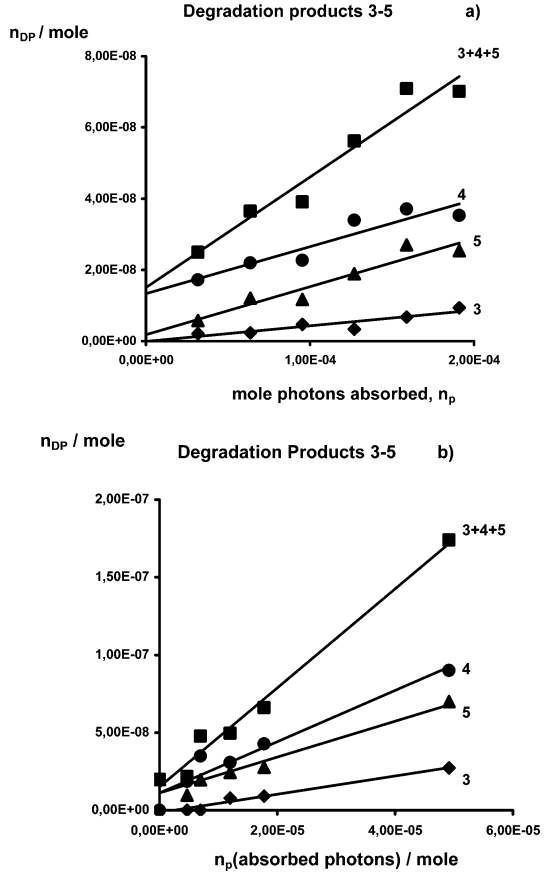

Figure 4. (a) Plot of the moles of each of degradation products **3**−**5** and the sum, n_{DP}, of products **3** + **4** + **5** as a function of the moles of absorbed photons, n_p, from extracted solutions of illuminated colloidal **N719**-dyed TiO_2 particles in deoxygenated acetonitrile: laser light intensity, 9.58 mW/cm²; method II; $n(\mathbf{3} + \mathbf{4} + \mathbf{5}) = (3.1 \times 10^{-4})n_p + 1.5 \times 10^{-8}$; $R^2 = 0.946$. (b) Tungsten−halogen lamp; 525-nm filter; light intensity, 0.10 mW/cm²; method I; $n(\mathbf{3} + \mathbf{4} + \mathbf{5}) = (3.2 \times 10^{-3})n_p + 1.5 \times 10^{-8}$; $R^2 = 0.948$.

expressions for the corrected rate of degradation, k^c_{deg} (see the Appendix).

$$k^u_{deg} = \Phi_{deg} k_{back}(I_0) \tag{9}$$

$$f_c = \frac{k^c_{deg}}{k^u_{deg}} = 0.60 \tag{10}$$

The mathematical treatment shows that f_c is a constant of 0.60 and does not depend on the incoming laser light intensity, I_0.

The results of all the photolysis experiments performed with both methods I and II are presented in Table 3. The applied light intensity, I_0, was 1−160 W/m², which is low relative to the 1000 W/m² intensity of standard AM1.5 solar illumination.

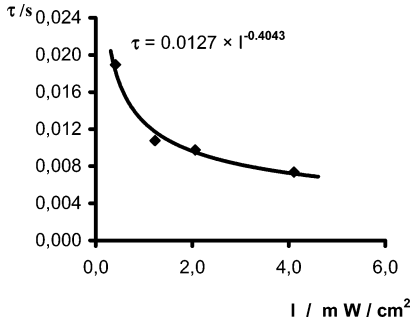

Figure 5. τ_{back} obtained by photoinduced absorption (PIA) measurements as a function of the laser light intensity. $\tau_{back} = 0.0127 \times I^{-0.4043}$.

In the applied intensity interval, k_{back} increases by a factor of 8 from 31 to 243 s^{-1}, while the measured Φ_{deg} decreases by a factor of 15 from 3×10^{-3} to 2×10^{-4}. The degradation rate of the $[Ru^{(III)}L_2(NCS)_2]^+$, k^c_{deg}, is reasonably constant, with an average value of $(4.0 \pm 1.0) \times 10^{-2}$ s^{-1}. Taking into consideration the large variation of the I_0 values and the application of two different experimental procedures (methods I and II), the relatively low standard deviation (≈20%) is quite remarkable. In method I the TiO_2 particles are sintered at 450 °C, producing large aggregates of TiO_2 particles, whereas in method II much smaller, nonsintered particles are used. The relatively constant k_{deg} values suggest that our simple kinetic scheme, eqs 1, 2, 4, and 5, does represent the chemistry of the photolysis experiments reasonably correctly.

The half-life, τ_{deg}, of $[Ru^{(III)}L_2(NCS)_2]^+$ attached to the TiO_2 surface is remarkably long ($\tau_{deg} = \ln 2/k_{deg} \approx 17$ s) compared to its half-life in acetonitrile, $\tau_{ACN} = 0.2$ ms, measured by using cyclic voltammetry experiments.[10] Apparently the attachment to the TiO_2 surface stabilizes, by some unknown mechanism, the Ru(III) form against oxidative degradation.

Determination of the Turnover Number in a DSSC. The turnover number, N, of the dye in a dye-sensitized solar cell may be calculated from eq 11, where k_3 is the regenerative electron-transfer reaction rate between the iodide ion and the $Ru^{(III)}$ complex (eq 3). In most solar cells the iodide ion concentration is 0.5 M.

$$N = \text{turnover number} = \frac{k_3[I^-]}{k_{deg}} \tag{11}$$

The regeneration rates, k_3, of **N719** attached to nanocrystalline TiO_2 have been obtained by several groups using the mean results of laser flash photolysis experiments.[27−28] An overview of the k_3 values presented in the literature is shown in Table 4. The results obtained by Haque,[27a] Pelet,[27b] and Heimer[27c] gave high values of k_3 with a mean value of 4.2×10^7 M^{-1} s^{-1}, whereas the k_3 values obtained by Kuciauskas[28a] and Montanari[28b]

TABLE 3: Oxidative Degradation Rates, k_{deg}, of N719 Attached to TiO_2 Particles

light source	I_0, mW/cm^2	τ,[a] s	k_{back},[b] s^{-1}	Φ_{deg}[c]	$10^2 k^u_{deg}$,[d] s^{-1}	$10^2 k^c_{deg}$,[e] s^{-1}
tungsten−halogen lamp [f,g]	0.10	3.22×10^{-2}	31	3.2×10^{-3}	9.9	5.9
halogen lamp [f,g]	0.54	1.63×10^{-2}	61	1.4×10^{-3}	8.3	5.0
laser [h,i]	0.93	1.31×10^{-2}	76	7.7×10^{-4}	5.6	3.3
laser	2.86	1.27×10^{-2}	120	5.5×10^{-4}	6.6	4.0
laser	4.65	6.82×10^{-3}	147	4.1×10^{-4}	6.0	3.6
laser	9.58	5.09×10^{-3}	196	3.1×10^{-4}	6.1	3.6
laser	6.79	5.85×10^{-3}	171	3.8×10^{-4}	6.4	3.9
laser	16.30	4.11×10^{-3}	243	2.0×10^{-4}	5.0	3.0
average ± sdv					6.7 ± 1.6	$\mathbf{4.0 \pm 1.0}$

[a] Measured using the PIA method. [b] $k_{back} = 1/\tau$. [c] Relative standard deviations of Φ_{deg} are between 6% and 15%. [d] Uncorrected degradation rates. [e] Corrected rates, see text. [f] 525 ± 10 nm, band-pass filter used. [g] Method 1 used. [h] $\lambda = 532$ nm. [i] Method 2 used.

TABLE 4: Regeneration Rates, k_3, of N3 Obtained from the Literature

ref	experimental conditions	k_3/M^{-1} s^{-1}	N[c]
Haque[27a]	0.3 M KI in propylene carbonate/ethylene carbonate[a]	2.3×10^7	2.8×10^8
Pelet[27b]	propylene carbonate, $[I^-] = 0.1$ M, $[Li^+] > 10^{-2}$ M[b]	3.6×10^7	4.5×10^8
Heimer[27c]	MeOH, 0.5 M NaI	7.1×10^7	8.9×10^8
Kuciauskas[28a]	CH_3CN, 0.5 M LiI	2.6×10^5	2.5×10^6
Montanari[28b]	propylene carbonate	1.6×10^5	2.0×10^6

[a] $t_{1/2} = 100$ ns, $k_3 = \ln 2/(t_{1/2} \times [I^-])$. [b] $1/t_{1/2} = 6 \times 10^6$ s^{-1}. [c] N calculated from eq 9 (see text).

are more than 200 times slower, with a mean value of $k_3 = 2.1 \times 10^5$ M^{-1} s^{-1}. It is not obvious to us why there is such a large divergence in the obtained regeneration rates. Based on the average of the two slowest regeneration rates obtained for **N719** and assuming that the degradation rate, $k_{deg} = 4.0 \times 10^{-2}$ s^{-1}, obtained for our simple model system is valid for a nc-DSSC, a turnover number N equal to 2.6×10^6 may be calculated with eq 9. This number corresponds to 0.5 years of normal solar cell operation, which is clearly insufficient for practical purposes. In contrast, when the average of the three highest values of k_3 is used, $N = 5.3 \times 10^8$ is obtained, indicating an **N719** sensitizer dye that is nearly perfectly stable under solar cell operation with respect to oxidative degradation. The corresponding solar cell lifetime would then be more than 20 years.

Our calculations of **N719** dye lifetimes are based on the assumption that the dye oxidative degradation rate, k_{deg}, under real nc-DSSC operation conditions is the same as that obtained from our simple model system. Observation of the same degradation products **3**−**5** as found in our model experiments from LC−UV−MS analysis of dye extracts of long-time illuminated complete dye sensitized solar cells[30] supports this assumption. Therefore, in a qualitative way our model system represents the more complex real nc-DSSC reasonably well. Hinsh et al. have reported nc-DSSC stability equivalent to 10 years of normal solar cell operation after 8300 h of light soaking at 2−5 sun.[14] This can be taken as an intrinsic stability of **N719** equivalent to at least 10 years, which is relatively close to the predicted lifetime based on our model system, applying the high average value of dye regeneration rate, k_3. The dye degradation kinetics based on our model system therefore seems to simulate the dye degradation kinetics in a real nc-DSSC reasonably well. Even though the dye degradation rates obtained from the simple model experiments may not be able to predict the lifetimes of solar cell dyes in real nc-DSSC better than within a factor of 2−3, the k_{deg} values may be used to rank the relative stability of various solar cell dyes in an experimentally simple and fast way. Investigations on dye degradation kinetics in real nc-DSSC are in progress.

Conclusion

The oxidative degradation rate, k_{deg}, of solar cell dye **N719** was obtained by applying a simple model system. Colloidal solutions of **N719**-dyed TiO_2 particles in acetonitrile were irradiated by 532-nm monochromatic light, and the sum of the quantum yields of the oxidative degradation products $[RuL_2(CN)_2]$, $[RuL_2(NCS)(CN)]$, and $[RuL_2(NCS)(ACN)]$, Φ_{deg}, were obtained at eight different light intensities in the range 0.1−16.30 mW/cm^2 by LC−UV−MS. The Φ_{deg} values decreased from 3.19×10^{-3} to 2×10^{-4} in the applied intensity range. By using the relation $k_{deg} = \Phi_{deg} k_{back}$ and back electron-transfer reaction rates, k_{back}, obtained from photoinduced absorption spectroscopy, it was possible to calculate an average value for the oxidative degradation rate of **N719** dye attached to the TiO_2 particles, $k_{deg} = 4.0 \times 10^{-2}$ s^{-1}. The stability of **N719** dye during solar cell operation was discussed, based on both this number and literature values of the regeneration reaction rate between $[Ru^{(III)}L_2(NCS)_2]$ and iodide. Five values for the **N719** dye regeneration rate constant, k_3, were found in the literature, the lowest and highest such values differing by more than a factor of 100. On the basis of the average of the three highest k_3 values, $N = 5.3 \times 10^8$ was obtained. This high turnover number indicates that an almost perfectly stable **N719** dye that could remain stable for more than 20 years under normal solar cell operating conditions, provided that oxidative degradation is the only route of dye degradation. A low value, $N = 2.6 \times 10^6$, was calculated based on the two lowest k_3 values corresponding to a lifetime of less than half a year under solar cell operation conditions. Obviously more measurements are needed to reach a consensus on the $Ru^{(II)}$ regeneration rate constant.

Appendix

The quantum yield of degradation, Φ, depends on the intensity of the absorbed light, I, according to eq A1. In this equation, k^c_{deg} is the rate of oxidative degradation of the Ru(III) state, and the back electron-transfer rate, $k_{back}(I)$, is given by eq A2, with $\alpha = 0.4043$. The experimentally obtained quantum yield, Φ, may be calculated as the average $\langle \Phi(I) \rangle$ over the intensity interval $[0, I_0]$ (see eq A3). Substitution of eqs A1 and A2 into eq A3 gives eq A4. The uncorrected rate of degradation, k^u_{deg}, is defined by eq A5. By inserting the expressions k^c_{deg} and k^u_{deg} (eqs A4 and A5) into the definition of f_c, a value close to 0.60 may be calculated (eq A6).

$$\Phi(I) = \frac{k_{\mathrm{deg}}^{\mathrm{u}}}{k_{\mathrm{back}}(I)} \tag{A1}$$

$$k_{\mathrm{back}} = \beta I^{\alpha} \tag{A2}$$

$$\Phi = \langle \Phi(I) \rangle = \frac{1}{I_0} \int_0^{I_0} \Phi(I)\, \mathrm{d}I \tag{A3}$$

$$\Phi = \frac{k_{\mathrm{deg}}^{\mathrm{c}}}{\beta I_0} \int_0^{I_0} I^{-\alpha}\, \mathrm{d}I = \frac{k_{\mathrm{deg}}^{\mathrm{c}}}{\beta} I_0^{-\alpha} \frac{1}{(1-\alpha)} \tag{A4}$$

$$\Phi = \frac{k_{\mathrm{deg}}^{\mathrm{u}}}{k_{\mathrm{back}}(I_0)} = \frac{k_{\mathrm{deg}}^{\mathrm{u}}}{\beta} I_0^{-\alpha} \tag{A5}$$

$$f_{\mathrm{c}} = \frac{k_{\mathrm{deg}}^{\mathrm{c}}}{k_{\mathrm{deg}}^{\mathrm{u}}} = (1-\alpha) = (1 - 0.4043) \approx 0.60 \tag{A6}$$

References and Notes

(1) O'Regan, B.; Grätzel, M. *Nature* **1991**, *353*, 737.

(2) Hagfeldt, A.; Grätzel, M. *Chem. Rev.* **1995**, *95*, 49.

(3) Grätzel, M. *Coord. Chem. Rev.* **1998**, *77*, 347.

(4) Hagfeldt, A.; Gratzel, M. *Acc. Chem. Res.* **2000**, *33*, 269.

(5) Vlachopoulos, N.; Liska, L.; Augustynski, J.; Grätzel, M. *J. Am. Chem. Soc.* **1988**, *110*, 1216.

(6) Nazeeruddin, M. K.; Kay, A.; Rodicio, I.; Humphry-Baker, R.; Müller, E.; Liska, P.; Vlachopoulos, N.; Grätzel, M. *J. Am. Chem. Soc.* **1993**, *115*, 6382.

(7) Kohle, O.; Grätzel, M.; Meyer, A. F.; Meyer, T. B. *Adv. Mater.* **1997**, *9*, 904.

(8) Grunwald, R.; Tributsch, H. *J. Phys. Chem. B* **1997**, *101*, 2564.

(9) Macht, B.; Turrión, M.; Barkschat, A.; Salvador, P.; Ellmer, K.; Tributsch, H. *Sol. Energy Mater. Sol. Cells* **2002**, *73*, 163.

(10) Cecchet, F.; Gioacchini, A. M.; Marcaccio, M.; Paolucci, F.; Roffia, S.; Alebbi, M.; Bignozzi, C. A. *J. Phys. Chem. B* **2002**, *106*, 3926.

(11) Hinsch, A.; Kroon, J. M.; van Roosmalen, J. A. M.; Bakker, N. J.; Sommeling, P.; van der Burg, N.; Kinderman, R.; Kern, R.; Feber, J.; Chill, C.; Schubert, M.; Meyer, A.; Meyer, T.; Uhlendorf, I.; Holzbock, J.; Niepmann, R. 16th European Photovoltaic Solar Energy Conference and Exhibition, Glasgow, 2000.

(12) Rijnberg, E.; Kroon, J. M.; Wienke, J.; Hinsch, A.; van Roosmalen, J. A. M.; Sinke, C.; Scholtens, B. J. R.; de Vries, J. G.; de Koster, C. G.; Duchateau, A. L. L.; Maes, I. C. H.; Henderickx, H. J. W. *Proc. World Confe. PVSEC 2nd* **1998**, 47.

(13) Nazeeruddin, Md. K.; Amirnasr, M.; Comte, P.; Mackay, J. R.; McQuillan, A. J.; Houriet, R.; Gratzel, M. *Langmuir* **2000**, *16*, 8525.

(14) Hinsch A.; Kroon, J. M.; Kern, R.; Uhlendorf, I.; Meyer, A.; Ferber, J. *Prog. Photovolt. Res.* **2001**, *9*, 425.

(15) Greijer, H. A.; Lindgren, J.; Hagfeldt, A. *J. Phys. Chem. B* **2001**, *105*, 6314.

(16) Greijer, H. A.; Lindgren, J.; Hagfeldt, A. *J. Photochem. Photobiol. A* **2004**, *164*, 23.

(17) Greijer-Agrell, H.; Lindgren, J.; Hagfeldt, A. *Solar Energy* **2003**, *75*, 169.

(18) Finnie, K. S.; Bartlett, J. R.; Woolfrey, J. L. *Langmuir* **1998**, *14*, 2744.

(19) (a) Kallioinen, J.; Lehtovuori, V.; Myllyperkiö, P.; Korppi-Tommola, J. *Chem. Phys. Lett.* **2001**, *340*, 217. (b) Tachibana, Y.; Haque, S. A.; Mercer, I. P.; Durrant, J. R.; Klug, D. R. *J. Phys. Chem. B* **2000**, *104*, 1198. (c) Ellingson, R. J.; Asbury, J. B.; Ferrere, S.; Ghosh, H. N.; Sprague, J. R.; Lian, T.; Nozik, A. J. *J. Phys. Chem. B* **1998**, *102*, 6455.

(20) (a) Kuciauskas, D.; Monat, J. E.; Villahermosa, R.; Gray, H. B.; Lewis, N. S.; McCusker, J. K. *J. Phys. Chem. B* **2002**, *106*, 9347. (b) Tachibana, Y.; Moser, J. E.; Gratzel, M.; Klug, D. R.; Durrant, J. R. *J. Phys. Chem.* **1996**, *100*, 20056. (c) Hannappel, T.; Burfeindt, B.; Storck, W.; Willig, F. *J. Phys. Chem. B* **1997**, *101*, 6799.

(21) (a) Nasr, C.; Hotchandani, S.; Kamat, P. V. *J. Phys. Chem. B* **1998**, *102*, 4944. (b) Alebbi, M.; Bignozzi, C. A.; Heimer, T. A.; Hasselmann, G. M.; Meyer, G. J. *J. Phys. Chem. B* **1998**, *102*, 7577.

(22) Fitzmaurice, D. J.; Frei, H. *Langmuir* **1991**, *7*, 1129.

(23) Amirnasr, M.; Nazeeruddin, Md. K.; Grätzel, M. *Thermochim. Acta* **2000**, *348*, 105.

(24) Bond, A. M.; Howitt, J.; MacFarlane, D. R.; Spiccia, L.; Wolfbauer, G. *J. Electrochem. Soc.* **1999**, *146*, 648.

(25) Das, S.; Kamat, P. V. *J. Phys. Chem. B* **1998**, *102*, 8954.

(26) Hansen, G.; Gervang, B.; Lund, T. *Inorg. Chem.* **2003**, *42*, 5545.

(27) (a) Haque, S. A.; Tachibana, Y.; Klug, D. R.; Durrant, J. R. *J. Phys. Chem. B* **1998**, *102*, 1745. (b) Pelet, S.; Moser, J.-E.; Gratzel, M. *J. Phys. Chem. B* **2000**, *104*, 1791. (c) Heimer, T. A.; Heilweil, E. J.; Bignozzi, C. A.; Meyer, G. J. *J. Phys. Chem. A* **2000**, *104*, 4256.

(28) (a) Kuciauskas, D.; Freund, M. S.; Gray, H. B.; Winkler, J. R.; Lewis, N. S. *J. Phys. Chem. B* **2001**, *105*, 392. (b) Montanari, I.; Nelson, J.; Durrant, J. R. *J. Phys. Chem. B* **2002**, *106*, 12203.

(29) Boschloo, G.; Hagfeldt, A. *Chem. Phys. Lett.* **2003**, *370*, 381.

(30) Lund, T. Manuscript in preparation.